

Revision 1

**Lusernaite-(Y), $Y_4Al(CO_3)_2(OH,F)_{11}\cdot 6H_2O$, a new
mineral species from Luserna Valley, Piedmont, Italy:
description and crystal structure**

CRISTIAN BIAGIONI¹, ELENA BONACCORSI¹, FERNANDO CÁMARA^{2,3},
MARCELLA CADONI^{2,3}, MARCO E. CIRIOTTI⁴, DANILO BERSANI⁵, UWE
KOLITSCH^{6,7}

¹ *Dipartimento di Scienze della Terra, Università di Pisa, Via S. Maria 53, I-56126 Pisa, Italy*

² *Dipartimento di Scienze della Terra, Università di Torino, Via Valperga Caluso 35, I-10125 Torino, Italy*

³ *CrisDi, Interdepartmental Centre for the Research and Development of Crystallography, Via P. Giuria 5, I-10125, Torino, Italy*

⁴ *Associazione Micro-mineralogica Italiana, Via San Pietro 55, I-10073 Devesi/Cirié, Torino, Italy*

⁵ *Dipartimento di Fisica, Università di Parma, Viale G.P. Usberti 7/a, I-43100 Parma, Italy*

⁶ *Mineralogisch-Petrographische Abt., Naturhistorisches Museum, Burgring 7, 1010 Wien, Austria*

⁷ *Institut für Mineralogie und Kristallographie, Geozentrum, Universität Wien, Althanstraße 14, 1090 Wien, Austria*

*e-mail address: biagioni@dst.unipi.it

23

24

ABSTRACT

25

26 The new mineral species lusernaite-(Y), ideally $Y_4Al(CO_3)_2(OH,F)_{11} \cdot 6H_2O$, has been discovered in
27 small fractures of the “Luserna Stone”, a leucocratic orthogneiss belonging to the Dora-Maira
28 massif, Western Alps, Italy. It occurs as colorless, thin platelets, with white streak and mica-like
29 pearly luster, elongated along [100] and flattened on {010}, arranged in radiating aggregates.
30 Lusernaite-(Y) is associated with aeschynite-(Y), albite, “chlorite”, hematite, pyrite, quartz, and
31 titanite. Lusernaite-(Y) has a perfect cleavage on {010} and a less marked one probably on {100}.
32 Its calculated density is $2.810 \text{ g} \cdot \text{cm}^{-3}$. In plane polarized light, it is transparent, with parallel
33 extinction and positive elongation. Lusernaite-(Y) is biaxial positive; its optical orientation is $\mathbf{a} = Z$,
34 $\mathbf{b} = X$, $\mathbf{c} = Y$. Owing to the crystal morphology, only two refractive indices could be measured,
35 corresponding to β 1.566(2) and γ 1.577(2).

36 Lusernaite-(Y) is orthorhombic, space group *Pmna*, with a 7.8412(3), b 11.0313(5), c 11.3870(4) Å,
37 V 984.96(7) Å³, $Z = 2$. Main diffraction lines of the X-ray powder diffraction pattern are [d in Å, (hkl)]:
38 11.02 (100) (010), 7.90 (49) (011), 5.66 (25) (002), 5.06 (24) (012), 4.258 (33) (112), 3.195
39 (27) (220), 3.095 (21) (212). Raman spectroscopy confirmed the presence of CO_3 groups (sharp
40 peak at 1096 cm^{-1}); due to the very strong luminescence, the bands of the OH and H_2O groups could
41 not be seen.

42 Chemical analyses by electron microprobe gave (wt%) Al_2O_3 6.11, Y_2O_3 43.52, La_2O_3 0.02, Ce_2O_3
43 0.04, Nd_2O_3 0.03, Sm_2O_3 0.16, Gd_2O_3 1.39, Dy_2O_3 3.46, Er_2O_3 3.15, Yb_2O_3 2.09, CaO 0.33, PbO
44 0.37, H_2O 22.76, CO_2 9.95, F 1.40, $O \equiv F$ -0.59, sum 94.19; H_2O and CO_2 were determined from
45 structure refinement. The empirical formula by assuming the presence of two $(CO_3)^{2-}$ groups,
46 eleven $(OH,F)^-$ anions, and six H_2O groups, in agreement with micro-Raman and structural results,
47 is $(Y_{3.41}Dy_{0.16}Er_{0.15}Yb_{0.09}Gd_{0.07}Ca_{0.06}Pb_{0.02}Sm_{0.01})_{\Sigma 3.97}Al_{1.06}(CO_3)_{2.00}(OH_{10.35}F_{0.65})_{\Sigma 11.00} \cdot 6H_2O$.

2

48 The crystal structure was solved by direct methods and refined on the basis of 840 observed
49 reflections to $R_1 = 6.8\%$. In the structure of lusernaite-(Y), yttrium and *REE* cations occupy two
50 distinct sites, Y1 and Y2, both in eight-fold coordination. The structure is built by layers parallel to
51 (010), formed by chains of edge-sharing Y-centered polyhedra (Y1), which run along [100], and are
52 connected along *c* through Al-centered octahedra. These chains are decorated on one side by
53 corner-sharing chains of Y-centered polyhedra (Y2), and on the other side by CO₃ groups. Along
54 [001] the decorated chains alternate their polarity.

55 Lusernaite-(Y), named after the type locality, the Luserna Valley, shows a new kind of structure
56 among the natural carbonates of *REE*. Its origin is related to the circulation of hydrothermal
57 solutions during the late-stage Alpine tectono-metamorphic events.

58

59 **Key words:** lusernaite-(Y), new mineral species, carbonate, yttrium, crystal structure, Luserna
60 stone, Piedmont, Italy.

61

62 INTRODUCTION

63 The “Luserna stone”, a leucocratic orthogneiss, has been quarried since the Middle Age and it is
64 an important building material for its widespread occurrence and use in historical monuments. The
65 first publications about this stone date back to the beginning of the 19th Century, with the studies of
66 Barelli (1835) and De Bartolomeis (1847), focused on the technological and economic importance
67 of the quarrying activities. The first scientific work can be considered that of Gastaldi (1874), who
68 tentatively reconstructed the lithostratigraphic setting of the “Luserna stone”. Since then, a large
69 number of studies about this stone have been published (Sandrone 2001). Surprisingly, only
70 recently the mineralogical peculiarities of this formation have been investigated. Vaccio (2002),
71 Piccoli et al. (2007), and Finello et al. (2007) described the minerals occurring in late-stage
72 fractures in the “Luserna stone”, reporting more than 40 different mineral species. A large number
73 of *REE* and Y phases were listed by the latter authors, including aeschynite-(Y), allanite-(Ce),
74 aluminocerite-(Ce), cerite-(Ce), fergusonite-(Y), hellandite-(Y), kainosite-(Y), monazite-(Ce),
75 synchysite-(Ce), xenotime-(Y), and probably polycrase-(Y). In addition, some unidentified minerals
76 have been described; among these, the mineral UK01, which corresponds to the new mineral
77 species lusernaite-(Y).

78 The new species and its name have been approved by the IMA-CNMNC (no. 2011-108). It is
79 named after the type locality, the Luserna Valley (Piedmont, Italy); the Levinson suffix (Bayliss and
80 Levinson 1988) indicates the dominance of Y among Y and *REE*. The type material is deposited in
81 the mineralogical collections of the Museo di Storia Naturale, University of Pisa, Via Roma 79,
82 Calci (Pisa, Italy) under the catalog number 19445. A cotype specimen is kept in the mineralogical
83 collections of the Museo Regionale di Scienze Naturali, Via Giovanni Giolitti 36, Torino (Italy),
84 with catalog number M/15901.

85

86 **GEOLOGICAL SETTING AND MINERAL OCCURRENCE**

87 The “Luserna stone” refers to a heterogeneous series of leucocratic gneisses (characterized
88 by a micro-*Augen* texture and grey-greenish or locally pale blue color) and phengitic schists,
89 cropping out in an area 50 km² wide in the Cottian Alps, at the border of the provinces of Torino
90 and Cuneo. This complex forms a flat body structurally located at the top of the Dora-Maira massif,
91 the southernmost of the so-called Internal Crystalline Massif of the Western Alps (Bussy and
92 Cadoppi 1996).

93 Whereas Vialon (1966) interpreted the “Luserna stone” as a metamorphosed volcano-
94 sedimentary sequence, other authors proposed a granitic origin on the basis of petrographic and
95 geochemical data (Cadoppi 1990; Bussy and Cadoppi 1996; Sandrone et al. 2004). The age of this
96 complex is still unknown; U-Pb dating on zircon indicates that most of the dated metagranites
97 belonging to the Dora-Maira massif were emplaced during the Upper Carboniferous, in relation
98 with the Variscan orogeny (Bussy and Cadoppi 1996).

99 Mineral assemblages and phase chemistry suggest an Alpine metamorphic evolution
100 characterized by an early eclogite-*facies* stage at pressures between 1.4 and 2.5 GPa for 550 ± 50°C;
101 this stage was overprinted by a greenschist-*facies* metamorphism during the exhumation of the
102 Dora-Maira massif at 35-40 My (Scaillet et al. 1992).

103 Mineralogically, the “Luserna stone” is composed of quartz (30-45 vol%), K-feldspar (10-25
104 vol%), albite (15-25 vol%), “phengite” (10-20 vol%), and subordinate “biotite”, “chlorite”, and
105 epidote-group minerals. Common accessories are opaque phases, titanite, “apatite”, and zircon;
106 locally, “tourmaline”, carbonates, “axinite”, and fluorite are also present (Sandrone et al. 2004).

107 Finello et al. (2007) described two kinds of mineral occurrence: *i*) in small fractures, normal
108 to the main field foliation, probably related to the late-stage tectonic events; and *ii*) in small aplite
109 dykes, parallel to the main foliation. Lusernaite-(Y) was found only in the first kind of occurrence.

110 Lusernaite-(Y) was found in the Seccarezze quarries (latitude 44°46'N, longitude 7°12'E),
111 Luserna San Giovanni, Torino, Piedmont, Italy. The first find of lusernaite-(Y) dates back to the

112 1991, when a mineral collector, G. Finello, found two specimens of a phase that proved to be a
113 possible new mineral species and was described as UK01 (UKGFN009Mugniv) by Finello *et al.*
114 (2007); a new find of better quality was made in 2006 by the mineral collectors B. Marelllo and C.
115 Alciati. Other findings of this rare mineral were done in October 2009 (about 15 specimens) and in
116 April-May 2010 (eight collected specimens). The new findings allowed a complete description of
117 the mineral and its approval as a new species. Finally, a last finding of lusernaite-(Y) occurred in
118 March 2012, as radial aggregates of well-developed tabular crystals, in one case associated with
119 calcite.

120 The crystallization of lusernaite-(Y) is probably related to the circulation of hydrothermal fluids
121 in late-stage fractures during the Tertiary Alpine tectono-metamorphic events.

122

123 **MINERALOGICAL CHARACTERIZATION**

124 *Appearance and physical properties*

125 Lusernaite-(Y) occurs as thin platelets, up to 1 mm in size, with an indistinct, roughly six-sided
126 outline. Crystals are elongated along **a** and flattened on {010} and are arranged in radiating
127 aggregates (Fig. 1). Associated minerals are aeschynite-(Y), albite, “chlorite”, hematite, pyrite,
128 quartz, and titanite.

129 Lusernaite-(Y) is colorless, with a white streak and a mica-like pearly luster. In plane polarized
130 light, it is transparent. Between crossed polars, the mineral shows parallel extinction, with a positive
131 elongation parallel to [100]. Birefringence is weak. It is optically biaxial positive, with a low value
132 of $2V$. The optical orientation is **a** = Z, **b** = X, **c** = Y. Due to the crystal morphology, only the two
133 refractive indices laying within the (010) plane could be measured in white light using the Becke
134 line method. The measured refractive indices are β 1.566(2) and γ 1.577(2). The mean refractive
135 index n of lusernaite-(Y), calculated using the Gladstone-Dale relationship (Mandarino 1979, 1981),
136 using the empirical formula obtained assuming the presence of stoichiometric CO₂ and H₂O (see
137 below), is 1.588. The difference between the measured values and the calculated mean refractive

138 index may be ascribed to chemical variations; for example, the greater the fluorine content, the
139 lower is the mean refractive index of lusernaite-(Y). In addition, other possible ionic substitution in
140 the cation sites (*e.g.*, differences in the relative abundance of *REE* and Y) may be invoked.

141 Density was not measured, due to the small crystal size and the difficulty in observing the
142 mineral in the heavy liquids; the calculated density, based on the empirical formula used for the
143 calculation of the mean refractive index, is $2.810 \text{ g}\cdot\text{cm}^{-3}$.

144 Lusernaite-(Y) is brittle, with a perfect {010} cleavage; another cleavage (probably on {100})
145 was observed normal to the crystal elongation. Owing to the difficulty in preparing a polished
146 surface and to the softness of the mineral, a reliable value of hardness could not be measured.

147

148 **CHEMICAL AND SPECTROSCOPIC DATA**

149 *Chemical Data*

150 Preliminary qualitative chemical analysis by energy-dispersive spectroscopy was performed
151 using a Phillips LX30 SEM, equipped with an EDAX DX4 system. It indicated that the only
152 elements with $Z > 8$ occurring in lusernaite-(Y) are Y, Al, F, and minor Dy, Gd, and Er.

153 Quantitative chemical data were collected using a JEOL JXA-8200 electron-microprobe, using
154 an acceleration voltage of 15 kV and a beam current of 5 nA. The beam size was set to 15 μm in
155 order to prevent (or limit) the deterioration of the crystal of lusernaite-(Y); notwithstanding this,
156 some surficial damage of the analyzed crystals was observed. Standards were (element, emission
157 line): anorthite ($\text{AlK}\alpha$, $\text{CaK}\alpha$), synthetic YPO_4 ($\text{YL}\alpha$), synthetic REEPO_4 set ($\text{LaL}\alpha$, $\text{CeL}\alpha$, $\text{DyL}\alpha$,
158 $\text{NdL}\alpha$, $\text{ErL}\alpha$, $\text{YbL}\alpha$, $\text{GdL}\alpha$, $\text{SmL}\alpha$), galena ($\text{PbM}\alpha$), synthetic RbMnF_3 ($\text{FK}\alpha$). Concentrations of the
159 *REE* were corrected for overlaps. Fluorine concentration was measured on the basis of the $\text{FK}\alpha$
160 peak height; consequently, its measure is probably not accurate, owing to the problems associated
161 with $\text{FK}\alpha$ peak shape and breadth:height variability (*e.g.*, Solberg 1982; Raudsepp 1995; Ottolini et
162 al. 2000).

163 Table 1 gives the weight concentrations obtained on a polished fragment of lusernaite-(Y). The
164 reported H₂O and CO₂ contents were estimated, in agreement with the results of the crystal structure
165 study, showing the presence of two (CO₃)²⁻ groups, eleven (OH,F)⁻ anions, and six H₂O groups per
166 formula unit (*pfu*). The low total, *i.e.* 94.19 wt%, could be attributed to the superficial damage of
167 the sample and to the difficulty in preparing a good quality polished surface.

168 The empirical formula of lusernaite-(Y), based on 23 anions *pfu*, is
169 (Y_{3.41}Dy_{0.16}Er_{0.15}Yb_{0.09}Gd_{0.07}Ca_{0.06}Pb_{0.02}Sm_{0.01})_{Σ3.97}Al_{1.06}(CO₃)_{2.00}(OH_{10.35}F_{0.65})_{Σ11.00}·6H₂O. The
170 empirical formula simplifies to Y₄Al(CO₃)₂(OH)₁₁·6H₂O, which requires (wt%) Y₂O₃ 56.61, Al₂O₃
171 6.39, CO₂ 11.03, H₂O 25.97, total 100.00.

172 Lusernaite-(Y) is slowly soluble in dilute 1:10 HCl, with the development of small gas bubbles,
173 in agreement with the occurrence of carbonate groups in its structure.

174

175 *Micro-Raman spectroscopy*

176 Unpolarized micro-Raman spectra (Fig. 2) were obtained on an unpolished crystal of lusernaite-
177 (Y) in nearly back-scattered geometry, with a Jobin-Yvon Horiba “Labram” apparatus, equipped
178 with a motorized *x-y* stage and an Olympus microscope with a 50× objective. The 632.8 nm line of
179 a He-Ne laser and the 473.1 nm line of a Nd:YAG laser were used. The minimum lateral and depth
180 resolution were set to a few micrometers. The system was calibrated using the 520.6 cm⁻¹ Raman
181 peak of silicon before each experimental session. Spectra were collected through multiple
182 acquisitions with single counting times ranging between 20 and 180 s. Both Raman spectra obtained
183 with 473.1 and 632.8 nm excitation lines are dominated by strong luminescence features, in the
184 form of many groups of sharp bands, superimposed on a broad band centered at about 570 nm. The
185 only features ascribable to a Raman band is the sharp peak at 1096 cm⁻¹, confirming the presence of
186 CO₃²⁻ groups in the structure.

187 The main luminescence peaks are located in the region between 560 and 590 nm; the strongest
188 ones are at 573, 576, and 582 nm. Other weaker groups of luminescence bands are visible in the
189 regions around 488 and 752 nm (using the 473.1 nm excitation) and 660 nm (using the 632.8 nm
190 line). Dy³⁺ could be the cause of these luminescence bands, except the broad ones (Gaft *et al.*
191 2005); this observation agrees with the fact that Dy³⁺ is the main substituent of Y³⁺, as shown by
192 EPMA data. Due to the strong luminescence, even in the region of the bending and stretching of O-
193 H bonds, no detectable Raman signals could be collected.

194

195 X-RAY CRYSTALLOGRAPHY AND CRYSTAL STRUCTURE DETERMINATION

196 The powder X-ray diffraction pattern of lusernaite-(Y) was obtained using a 114.6 mm
197 Gandolfi camera and Ni-filtered CuK α radiation (Table 2). Indexing of the reflections was based on
198 a calculated powder pattern obtained by the structural model described below, using the software
199 POWDERCELL (Kraus and Nolze 1996). The unit-cell parameters refined from the powder data
200 with the software UNIT CELL (Holland and Redfern 1997), on the basis of 24 univocally indexed
201 reflections, are a 7.839(2), b 11.023(2), c 11.383(2) Å, V 983.6(2) Å³.

202 Preliminary Weissenberg photographs were obtained using a small crystal of lusernaite-(Y)
203 and allowed the morphological orientation of the crystal.

204 Single-crystal X-ray diffraction data were collected using an Oxford Gemini R Ultra
205 diffractometer equipped with a CCD area detector at CrisDi (Interdepartmental Centre for the
206 Research and Development of Crystallography, Torino, Italy). Graphite-monochromatized MoK α
207 radiation was used. Crystal data and experimental details are reported in Table 3. Some 763 frames
208 were collected in 1.0° slices between ω angles 3.57° and 33.49°. The exposure time was 130 s per
209 frame. Data were integrated and corrected for Lorentz and polarization, background effects, and
210 absorption, using the package CRYSTALIS^{Pro} (Oxford Diffraction 2007a, b). Refinement of the unit-
211 cell parameters was based on all measured reflections with $I > 200\sigma(I)$. At room temperature, the
212 unit-cell parameters are a 7.8412(3), b 11.0313(5), c 11.3870(4) Å, V 984.96(7) Å³, space group

9

213 *Pmna*, $Z = 2$. The $a:b:c$ ratio is 0.711:1:1.032. A total of 1081 independent reflections were
214 collected and the structure was solved and refined by means of the SHELX set of programs
215 (Sheldrick 2008).

216 After having located the Y and Al atoms, the structure was completed through successive
217 difference-Fourier maps. The latter showed the presence of two maxima around one of the two Y-
218 centered sites, *i.e.*, Y1, at 0.80 and 0.98 Å, respectively. On the basis of chemical data, these
219 residuals were attributed to Pb, lowering significantly the R values.

220 The refined occupancies of the Y1, Y2, Pb1a, and P1b sites were $Y_{0.370(8)}Er_{0.116(8)}$,
221 $Y_{0.457(7)}Dy_{0.043(7)}$, $Pb_{0.007(1)}$, and $Pb_{0.007(1)}$, respectively. This indicates that the other *REE* measured
222 by EPMA prefer to occupy Y1 and Y2 sites. The two refined Pb occupancies would equal to a Pb
223 content of ~ 0.06 *apfu*, a value which is higher than the measured value of 0.015 Pb *pfu*. Thus, it
224 may also be possible that some of the measured *REE*, which have ionic radii fairly different from
225 that of Y^{3+} (*e.g.*, Gd^{3+} , Yb^{3+}), may reside in these satellite positions.

226 Furthermore, some unacceptably short Pb- ϕ distances are observed, *e.g.*, Pb1a – O2
227 1.83(3)Å and Pb1b – O6 2.03(1) Å, and the actual coordination of these split sites cannot be
228 assessed. The total refined site scattering value at the Y1+Y2 sites is 176.5 e^- , to be compared with
229 167.8 e^- obtained from the chemical data. Two hydrogen positions were located in the difference-
230 Fourier maps; these hydrogen atoms were added to the model but their coordinates and isotropic
231 displacement parameters were not refined. Examination of the bond-valence balance and the
232 hydrogen bonds suggested that two O sites, namely O4 and O5, are possible F-bearing sites. A
233 lower R value was achieved by introducing fluorine at the O4 site. The O:F ratio in the O4 site was
234 fixed taking into account the EPMA data.

235 Refinement converged to $R_1 = 6.82\%$ for 840 observed reflections and 90 parameters. The
236 largest peak and hole in the final difference Fourier map are 2.67 and -1.09 $e \text{ \AA}^{-3}$, respectively.
237 Tables 4 and 5 report the atomic coordinates and displacement parameters, and selected bond
238 distances, respectively.

239

240 DESCRIPTION AND DISCUSSION OF THE STRUCTURE

241 *General features and cation coordination*

242 The crystal structure of lusernaite-(Y) (Fig. 3) is layered on (010); layering is a common
243 feature of (Y, REE) carbonates (Grice et al. 1994; Grice et al. 2007). In lusernaite-(Y) only one kind
244 of layer occurs; it is composed by two independent Y-centered polyhedra, one Al-centered
245 octahedron, one C-centered triangle, six anion positions, and three H₂O groups.

246 The two Y-centered sites, namely Y1 and Y2, are eight-fold coordinated. The average Y-φ
247 bond-lengths are 2.387 and 2.349 Å for Y1 and Y2 sites, respectively, with single values ranging
248 from 2.267 (Y2-O4 bond) to 2.486 (Y1-O5 bond) Å. Probably Pb occupies two sub-positions,
249 owing to its stereochemical activity; similar behavior has been observed for lead replacing
250 potassium in synthetic Pb₂(Pb,K)₄[Si₈O₂₀]O (Moore et al. 1985) and lead replacing barium in
251 hyalotekite (Moore et al. 1982; Christy et al. 1998). Aluminum is octahedrally coordinated, with an
252 average bond-length of 1.898 Å. The planar carbonate groups (CO₃) are inclined with respect to the
253 overall structural layering; they are attached through corner-sharing to two Y1-centered polyhedra.

254 The (010) layer is built by chains of edge-sharing Y-centered polyhedra (Y1 site), which run
255 along [100], and are connected along [001] through Al-centered octahedra. These chains are
256 decorated on one side by corner-sharing chains of Y-centered polyhedra (Y2 site), and on the other
257 side by CO₃ groups. Along [001] the decorated chains alternate their polarity. The (010) layers are
258 stacked along [010] by hydrogen bonding (see next section).

259

260 *Hydrogen bonding in lusernaite-(Y)*

261 The calculation of the bond-valence sums (BVS) for the nine independent anion sites (Table
262 6) gives values significantly different from 2 valence units (*vu*) for all these sites. Examination of
263 the O···O distances shorter than 3.0 Å (Table 7) suggests the presence of hydrogen bonds.

264 The undersaturation of O2 and O3 oxygen atoms, both bonded to CO₃ groups, is removed by
265 their probable hydrogen bonding; O2 is linked to O1 (hosting an OH group), whereas O3 is bonded
266 to O6 (hosting an OH group) and Ow1 (hosting a H₂O group). By applying the equation proposed
267 by Ferraris and Ivaldi (1988), their BVS increase up to 1.99 and 2.01 *vu*, indicating their population
268 by oxygen atoms. An additional O2...Ow3 hydrogen bond will be discussed below.

269 O1 and O6 sites, with BVS of 0.99 and 1.04 *vu*, respectively, are occupied by hydroxyl
270 anions, as the O4 and O5 sites. Moreover, the two latter sites are not involved in any plausible
271 hydrogen bond, and they could therefore host also fluorine atoms.

272 The Ow1 site is occupied by an H₂O group, which is involved in two hydrogen bonds: the
273 Ow1...O3 bond and the Ow1...Ow1' bond, with the two Ow1 sites belonging to successive layers
274 along [010]. The two hydrogen atoms located during the crystal structure determination, namely H1
275 and H2, are at 1.09 and 1.08 Å from Ow1. These bond lengths are a little longer than the expected
276 ones, but taking into account the quality of the refinement and the possible disorder affecting the
277 hydrogen-bond scheme, they could be retained as acceptable. Owing to the presence of a mirror
278 plane, H1 is statistically bonded to the Ow1 of the upper or the lower layer; the H2 takes part in the
279 Ow1-O3 bond. The H1 – Ow1 – H2 bond angle is *ca.* 98°.

280 A more complex situation occurs at the Ow2 and Ow3 sites. The Ow2 site is at 2.75(4) Å
281 from Ow3. The latter has a refined electron density indicating half occupancy. Figure 4 illustrates a
282 possible hydrogen-bonding scheme involving the Ow2 and Ow3 sites. Along [100], every two
283 Ow2, one acts as donor in Ow2...Ow3 hydrogen bond, the other as acceptor. Consequently, the
284 Ow2 site will be occupied, along **a**, by a regular alternation of H₂O and OH⁻ groups. Owing to the
285 lack of any correlation between adjacent columns, the Ow2 site will be statistically occupied by
286 H₂O and OH⁻. In addition, Ow3 is at 2.91(4) Å from two O2 sites. The angle between
287 O2...Ow3...Ow2 is *ca.* 114° and agrees with an hydrogen bond. It is possible that only one of the
288 two O2 sites is involved in a hydrogen bond with Ow3. In this way, O2 could be slightly
289 oversaturated, with a BVS of 2.13 *vu*, whereas Ow3 displays a negative BVS, *i.e.* -0.15 *vu*. The

290 deviation from an ideal valence sum could be related to the disorder occurring along [100], with the
291 statistically occupied Ow3 site probably representing an average position.

292 In conclusion, hydrogen bonds in lusernaite-(Y) are very important in assuring the link
293 between successive (010) layers, in agreement with its perfect {010} cleavage; the hydrogen bonds
294 linking successive layers are Ow1...Ow1 and, probably, Ow3...O2.

295

296 *Crystal chemistry of lusernaite-(Y)*

297 Crystal-structure determination and bond-valence analysis indicate that Y1 is coordinated by
298 two oxygen anions and six hydroxyl groups, Y2 is bonded to five (OH,F) anions, two H₂O groups,
299 and a mixed (H₂O/OH) site; Al is octahedrally coordinated by six hydroxyl groups.

300 Consequently, the layer of lusernaite-(Y) has a composition Y₄Al(CO₃)₂(OH,F)₁₁·5H₂O,
301 being electrostatically neutral; thus the net charge of the interlayer must be zero. In fact, adjacent
302 layers are connected through hydrogen bonding, involving also an additional water molecule, giving
303 the actual formula of lusernaite-(Y), Y₄Al(CO₃)₂(OH,F)₁₁·6H₂O.

304 The substitution of (Y,REE)³⁺ by (Pb,Ca)²⁺ yields a deficit of charges, compensated through
305 other compositional variation. Taking into account the crystal chemistry of lusernaite-(Y), the most
306 probable mechanism could involve the Ow2 site, *i.e.* the site with the mixed occupancy by OH⁻ and
307 H₂O groups. Electrostatic neutrality could be achieved through the coupled substitution



309 Other possible substitution mechanisms (*e.g.*, the substitution of trivalent Y and REE by Pb²⁺ and a
310 tetravalent cation) are less possible and cannot be proven.

311

312 **SUMMARY AND CONCLUSION**

313 With the discovery of lusernaite-(Y), twenty natural yttrium carbonates are known (Table 8).
314 No yttrium carbonates without additional anions and without H₂O (group 5.A) have been described
315 till now. Lusernaite-(Y), being a carbonate with additional anions and with H₂O, belongs to the 5.D

316 group of Strunz & Nickel (2001). It displays a new kind of layered crystal structure, with an
317 interlayer hosting H₂O molecules; it is also the first natural Y-Al carbonate.

318 Yttrium carbonates are usually found as late-stage hydrothermal phases in alkaline
319 magmatic rocks (or their metamorphic derivatives); in some cases, they occur in the oxidation zone
320 of U or Cu deposits. The occurrence of lusernaite-(Y) agrees with the usual genesis of these phases;
321 in fact, it occurs in late-stage fractures as product of hydrothermal activity related to the Alpine
322 tectono-metamorphic events. Owing to the richness of rare minerals in the fractures of the Luserna
323 stone, the quarries exploiting this kind of rock are an interesting field of research for the collection
324 and the study of the crystal chemistry of yttrium and *REE* minerals.

325

326 **ACKNOWLEDGEMENTS**

327 The authors wish to thank the mineral collector Bruno Marellò who provided us with the
328 first studied specimens; additional samples, useful for the completion of the study, were provided
329 by Giuseppe Finello and Graziano Del Core.

330 The comments of the Associate Editor Fernando Colombo and the referees Miguel Galliski,
331 Ron Peterson, and Jirí Sejkora help us in improving the paper.

332 Andrea Risplendente (Dipartimento di Scienze della Terra “Ardito Desio”, Milano, Italy) is
333 acknowledged for his assistance during electron-microprobe analysis. Chemical analysis of *REE*
334 were performed using a protocol made by Valeria Diella, National Research Council, Institute of
335 Environmental Processes. Carmelo Sibio (Dipartimento di Scienze della Terra, Torino, Italy) and
336 Italo Campostrini (Dipartimento di Chimica Strutturale e Stereochimica Inorganica, Milano, Italy)
337 are thanked for careful preparation of the polished crystals of lusernaite-(Y). Finally, Massimo
338 D’Orazio (Dipartimento di Scienze della Terra, Pisa, Italy) helped us in the optical characterization
339 of lusernaite-(Y).

340 **References**

- 341 Barelli, V. (1835) Cenni di statistica mineralogica degli Stati di S.M. il Re di Sardegna ovvero
342 Catalogo ragionato della raccolta formatasi presso l'Azienda Generale dell'Interno. Fordratto,
343 Torino, 687 pp. (in Italian).
- 344 Bayliss, P. and Levinson, A.A. (1988) A system of nomenclature for rare-earth mineral species:
345 Revision and extension. American Mineralogist, 73, 422-423.
- 346 Brese, N.E. and O'Keeffe, M. (1991) Bond-valence parameters for solids. Acta Crystallographica,
347 B47, 192-197.
- 348 Bussy, F. and Cadoppi, P. (1996) U-Pb dating of granitoids from the Dora-Maira massif (western
349 Italian Alps). Schweizerische Mineralogische und Petrographische Mitteilungen, 76, 217-233.
- 350 Cadoppi, P. (1990) Geologia del basamento cristallino nel settore settentrionale del Massiccio Dora-
351 Maira (Alpi Occidentali). Ph.D. Thesis, University of Torino, Italy, 201 pp (in Italian).
- 352 Chao, G.Y., Mainwaring, P.R. and Baker, J. (1978) Donnayite, $\text{NaCaSr}_3\text{Y}(\text{CO}_3)_6 \cdot 3\text{H}_2\text{O}$, a new
353 mineral from Mont Saint-Hilaire, Québec. Canadian Mineralogist, 16, 335-340.
- 354 Christy, A.G., Grew, E.S., Mayo, S.C., Yates, M.G. and Belakovskiy, D.I. (1998) Hyalotekite,
355 $(\text{Ba,Pb,K})_4(\text{Ca,Y})_2\text{Si}_8(\text{B,Be})_2(\text{Si,B})_2\text{O}_{28}\text{F}$, a tectosilicate related to scapolite: new structure
356 refinement, phase transitions and a short-range ordered *3b* superstructure. Mineralogical
357 Magazine, 62, 77-92.
- 358 De Bartolomeis, L. (1847) Notizie topografiche e statistiche sugli Stati Sardi. Tipografia Chirio e
359 Mina, Torino, 712 pp (in Italian).
- 360 Deliens, M. and Piret, P. (1986) La kamotoïte-(Y), un nouveau carbonate d'uranyle et de terres
361 rares de Kamoto, Shaba, Zaïre. Bulletin de Minéralogie, 109, 643-647.
- 362 Ferraris, G. and Ivaldi, G. (1988) Bond valence vs bond length in $\text{O}\cdots\text{O}$ hydrogen bonds. Acta
363 Crystallographica, B44, 341-344.

- 364 Finello, G., Ambrino, P., Kolitsch, U., Ciriotti, M.E., Blass, G. and Bracco, R. (2007) I minerali
365 della “Pietra di Luserna”, Piemonte, Italia Nord-Occidentale. I. Alcune cave di gneiss della
366 Val Luserna. MICRO, 2007, 181-226 (in Italian).
- 367 Gaft, M., Reisfeld, R. and Panczer, G. (2005) Modern luminescence spectroscopy of minerals and
368 materials. Springer, 374 pp.
- 369 Gastaldi, B. (1874) Studii geologici sulle Alpi Occidentali. Parte II. Memorie descrittive della Carta
370 Geologica d’Italia, 2, 3-61 (in Italian).
- 371 Grice, J.D. (1996) The crystal structure of shomiokite-(Y). Canadian Mineralogist, 34, 649-655.
- 372 Grice, J.D. and Chao, G.Y. (1997) Horváthite-(Y), rare-earth fluorocarbonate, a new mineral
373 species from Mont Saint-Hilaire, Quebec. Canadian Mineralogist, 35, 743-749.
- 374 Grice, J.D. and Gault, R.A. (1998) Thomasclarkite-(Y), a new sodium – rare earth-element
375 bicarbonate. Canadian Mineralogist, 36, 1293-1300.
- 376 Grice, J.D., Gault, R.A. and Chao, G.Y. (1995) Reederite-(Y), a new sodium rare-earth carbonate
377 mineral with a unique fluorosulfate anion. American Mineralogist, 80, 1059-1064.
- 378 Grice, J.D., Gault, R.A., Roberts, A.C. and Cooper, M.A. (2000) Adamsite-(Y), a new sodium-
379 yttrium carbonate mineral species from Mont Saint-Hilaire, Quebec. Canadian Mineralogist,
380 38, 1457-1466.
- 381 Grice, J.D., Maisonneuve, V. and Leblanc, M. (2007) Natural and synthetic fluoride carbonates.
382 Chemical Reviews, 107, 114-132.
- 383 Grice, J.D., Van Velthuisen, J. and Gault, R.A. (1994) Petersenite-(Ce), a new mineral from Mont
384 Saint-Hilaire, and its structural relationship to other REE carbonates. Canadian Mineralogist,
385 32, 405-414.
- 386 Holland, T.J.B. and Redfern, S.A.T. (1997) Unit cell refinement from powder diffraction data: the
387 use of regression diagnostics. Mineralogical Magazine, 61, 65-77.

- 388 Khomyakov, A.P., Polezhaeva, L.I., Yamnova, N.A. and Pushcharovsky, D.Yu. (1992) Mineevite-
389 (Y), $\text{Na}_{25}\text{Ba}(\text{Y,Gd,Dy})_2(\text{CO}_3)_{11}(\text{HCO}_3)_4(\text{SO}_4)_2\text{F}_2\text{Cl}$: a new mineral. Zapiski Vserossijskogo
390 Mineralogicheskogo Obshchestva, 121, 138-143 (in Russian).
- 391 Kraus, W. and Nolze, G. (1996) POWDER CELL – a program for the representation and
392 manipulation of crystal structures and calculation of the resulting X-ray powder patterns.
393 Journal of Applied Crystallography, 29, 301-303.
- 394 Li, Y., Burns, P.C. and Gault, R.A. (2000) A new rare-earth-element uranyl carbonate sheet in the
395 structure of bijvoetite-(Y). Canadian Mineralogist, 38, 153-162.
- 396 Mandarino, J.A. (1979) The Gladstone-Dale relationship. Part III. Some general applications.
397 Canadian Mineralogist, 17, 71-76.
- 398 Mandarino, J.A. (1981) The Gladstone-Dale relationship. Part IV. The compatibility concept and its
399 application. Canadian Mineralogist, 19, 441-450.
- 400 Milton, C., Ingram, B., Clark, J.R. and Dwornik, E.J. (1965) Mckelveyite, a new hydrous sodium
401 barium rare-earth uranium carbonate mineral from the Green River Formation, Wyoming.
402 American Mineralogist, 50, 593-612.
- 403 Mineev, D.A., Lavrishcheva, T.I. & Bykova, A.V. (1970) Yttrian bastnaesite, a product of the
404 alteration of gagarinite. Zapiski Vserossijskogo Mineralogicheskogo Obshchestva, 99, 328-
405 332 (in Russian).
- 406 Miyawaki, R., Kuriyama, J. and Nakai, I. (1993) The redefinition of tenerite-(Y), $\text{Y}_2(\text{CO}_3)_3 \cdot 2$ -
407 $3\text{H}_2\text{O}$, and its crystal structure. Canadian Mineralogist, 78, 425-432.
- 408 Moore, P.B., Araki, T. and Ghose, S. (1982) Hyalotekite, a complex lead borosilicate: its crystal
409 structure and the lone-pair effect of Pb(II). American Mineralogist, 67, 1012-1020.
- 410 Moore, P.B., Sen Gupta, P.K. and Schlemper, E.O. (1985) Solid solution in plumbous potassium
411 oxysilicate affected by interaction of a lone pair with bond pairs. Nature, 318, 548.
- 412 Nagashima, K., Miyawaki, R., Takase, J., Nakai, I., Sakurai, K., Matsubara, S., Kato, A. and Iwano,
413 S. (1986) Kimuraite, $\text{CaY}_2(\text{CO}_3)_4 \cdot 6\text{H}_2\text{O}$, a new mineral from fissures in an alkali olivine

- 414 basalt from Saga Prefecture, Japan, and new data on lokkaite. *American Mineralogist*, 71,
415 1028-1033.
- 416 Ottolini, L., Cámara, F. and Bigi, S. (2000) An investigation of matrix effects in the analysis of
417 fluorine in humite-group minerals by EPMA, SIMS, and SREF. *American Mineralogist*, 85,
418 89-102.
- 419 Oxford Diffraction (2007a) *CrysAlis CCD*. Oxford Diffraction Ltd, Abingdon.
- 420 Oxford Diffraction (2007b) *CrysAlis RED*. Oxford Diffraction Ltd, Abingdon.
- 421 Pekov, I.V., Chukanov, N.V., Zubkova, N.V., Ksenofontov, D.A., Horváth, L. Zadov, A.E. and
422 Pushcharovsky, D.Y. (2010) Lecoqite-(Y), $\text{Na}_3\text{Y}(\text{CO}_3)_3 \cdot 6\text{H}_2\text{O}$, a new mineral species from
423 Mont Saint-Hilaire, Quebec, Canada. *Canadian Mineralogist*, 48, 95-104.
- 424 Perttunen, V. (1970) Lokkaite, a new hydrous RE-carbonate from Pyörönmaa pegmatite in
425 Kangasala, S.W. Finland. *Bulletin of the Geological Society of Finland*, 43, 67-72.
- 426 Piccoli, G.C., Maletto, G., Bosio, P. and Lombardo, B. (2007) Minerali del Piemonte e della Valle
427 d'Aosta. Associazione Amici del Museo 'F. Eusebio', Alba, 610 pp. (In Italian).
- 428 Raade, G. and Brastad, K. (1993) Kamphaugite-(Y), a new hydrous Ca-(Y,REE)-carbonate mineral.
429 *European Journal of Mineralogy*, 5, 679-683.
- 430 Raudsepp, M. (1995) Recent advances in the electron-probe micro-analysis of minerals for the light
431 elements. *Canadian Mineralogist*, 33, 203-218.
- 432 Sandrone, R. (2001) La Pietra di Luserna nella letteratura tecnico-scientifica. In *Atti del Seminario*
433 *Internazionale su "Le Pietre Ornamentali della Montagna Europea"*, Luserna San Giovanni –
434 Torre Pellice (TO), 10-12 giugno 2001, 333-339 (in Italian).
- 435 Sandrone, R., Colombo, A., Fiora, L., Fornaro, M., Lovera, E., Tunesi, A. and Cavallo, A. (2004)
436 Contemporary natural stones from the Italian western Alps (Piedmont and Aosta Valley
437 Regions. *Periodico di Mineralogia*, 73, 211-226.
- 438 Scaillet, S., Feraud, G., Balleve, M. and Amouric, M. (1992) Mg/Fe and [(Mg,Fe)Si-Al₂]
439 compositional control on argon behaviour in high-pressure white micas: A $^{40}\text{Ar}/^{39}\text{Ar}$

- 440 continuous laser-probe study from the Dora-Maira nappe of the internal western Alps, Italy.
441 *Geochimica et Cosmochimica Acta*, 56, 2851-2872.
- 442 Sheldrick, G.M. (2008) A short history of SHELX. *Acta Crystallographica*, A64, 112-122.
- 443 Solberg, T.N. (1982) Fluorine electron microprobe analysis: variations of X-ray peak shape. In
444 *Microbeam Analysis* (K.F.J. Heinrich, ed.). San Francisco Press, Inc., San Francisco,
445 California (148-150).
- 446 Strunz, H. & Nickel, E.H. (2001) *Strunz Mineralogical Tables*. 9th edition. E. Schweizerbart Verlag,
447 Stuttgart, 870 pp.
- 448 Takai, Y. and Uehara, S. (2011) Hizenite-(Y), IMA 2011-030. CNMNC Newsletter No. 10, October
449 2011, page 2555. *Mineralogical Magazine*, 75, 2549-2561.
- 450 Vaccio, R. (2002) Cave di «Pietra di Luserna» nel territorio di Bagnolo. In Piccoli, G.C., *Minerali*
451 *delle Alpi Marittime e Cozie*. Provincia di Cuneo. Amici del Museo «F. Eusebio», Ed., Alba,
452 66-76 (in Italian).
- 453 Vialon, P. (1966) Etude géologique du Massif Dora-Maira (Alpes Cottiennes internes – Italie).
454 *Travaux du Laboratoire Géologique de Grenoble*, 4, 1-293 (in French).
- 455 Wallwork, K., Kolitsch, U., Pring, A. and Nasdala, L. (2002) Decrespignyite-(Y), a new copper
456 yttrium rare earth carbonate chloride hydrate from Paratoo, South Australia. *Mineralogical*
457 *Magazine*, 66, 181-188.
- 458 Wang, L. and Zhou, K. (1995) The crystal structure of synchysite-(Y), $YCa(CO_3)F$. *Acta*
459 *Petrologica et Mineralogica*, 14, 336-344 (in Chinese with English abs.).
460
461
462

463 **Table captions**

464 **Table 1** – Microprobe analyses of lusernaite-(Y): chemical composition as wt.% (average $n = 18$)
465 and number of atoms on the basis of $(O+F) = 23$ *apfu*, assuming the presence of 2 (CO_3) and 6 H_2O
466 groups *pfu*.

467 **Table 2** – Measured X-ray powder diffraction data for lusernaite-(Y).

468 **Table 3** – Crystal data and summary of parameters describing data collection and refinement for
469 lusernaite-(Y).

470 **Table 4** – Atomic coordinates and displacement parameters for lusernaite-(Y).

471 **Table 5** – Selected bond distances (in Å) in lusernaite-(Y).

472 **Table 6** – Bond-valence calculations for lusernaite-(Y), according to Brese & O’Keeffe (1991).

473 **Table 7** – $O\cdots O$ distances (in Å) in the suggested hydrogen-bonding scheme, with corresponding
474 bond-valence values (*vu*).

475 **Table 8** – Comparison of natural yttrium carbonates.

476

477 **Figure captions**

478 **Figure 1** – Colourless thin tabular crystals of lusernaite-(Y) associated with “chlorite”. Crystal
479 aggregate size: 2 mm. Collection and photo B. Marelllo.

480 **Figure 2** – Micro-Raman spectra of lusernaite-(Y) between 200 and 1200 cm^{-1} (a) and the effect of
481 luminescence (b) for both 473.1 and 632.8 nm excitation lines.

482 **Figure 3** – Crystal structure of lusernaite-(Y), as seen down [100] (a) and [010] (b). Polyhedra: dark
483 grey = Y-centered polyhedra; light grey = Al-centered octahedra; black = CO_3 groups. Balls: dark
484 grey = O^{2-} or $(OH,F)^-$ anions; light grey = H_2O molecules or mixed H_2O/OH^- occupied site.

485 **Figure 4** – The possible hydrogen bonds connecting successive (010) layers. Polyhedra: dark grey:
486 Y-centered polyhedra; light grey: Al-centered octahedra; black = CO₃ groups. Balls: dark grey: O2
487 sites; grey: Ow1, Ow2, Ow3 sites.

488

489

490

491 **Table 1** – Microprobe analyses of lusernaite-(Y): chemical composition as wt.% (average $n = 18$)
 492 and number of atoms on the basis of $(O+F) = 23$ *apfu*, assuming the presence of 2 (CO_3) and 6 H_2O
 493 groups *pfu*.
 494
 495

Oxide	wt.% (average $n = 18$)	range	e.s.d.	<i>apfu</i> (based on 23 anions)
Al ₂ O ₃	6.11	5.94 – 6.45	0.13	1.060
Y ₂ O ₃	43.52	42.28 – 44.69	0.77	3.410
La ₂ O ₃	0.02	0.00 – 0.12	0.03	0.002
Ce ₂ O ₃	0.04	0.00 – 0.16	0.05	0.002
Nd ₂ O ₃	0.03	0.00 – 0.12	0.03	0.002
Sm ₂ O ₃	0.16	0.00 – 0.37	0.10	0.008
Gd ₂ O ₃	1.39	1.06 – 1.66	0.15	0.068
Dy ₂ O ₃	3.46	2.97 – 3.77	0.19	0.164
Er ₂ O ₃	3.15	2.84 – 3.61	0.20	0.146
Yb ₂ O ₃	2.09	1.75 – 2.53	0.25	0.094
CaO	0.33	0.16 – 0.58	0.12	0.052
PbO	0.37	0.19 – 0.57	0.12	0.015
F	1.40	1.19 – 1.52	0.08	0.652
H ₂ O*	22.76			6 H ₂ O 10.348 OH ⁻
CO ₂ *	9.95			2.000
Subtotal	94.78			
Les O ≡ F	-0.59			
Total	94.19			

496

497 **Table 2** – Measured X-ray powder diffraction data for lusernaite-(Y).

l_{obs}	d_{meas} (Å)	l_{calc}	d_{calc} (Å)	$h k l$	l_{obs}	d_{meas} (Å)	l_{calc}	d_{calc} (Å)	$h k l$
vs	11.02	100	11.03	0 1 0	w	2.901	11	2.904	1 2 3
s	7.90	49	7.92	0 1 1	w	2.790	15	2.787	2 2 2
m	6.41	15	6.46	1 0 1	vw	2.667*			
m	5.66	25	5.69	0 0 2	vw	2.606	4	2.611	2 3 1
mw	5.06	24	5.06	0 1 2	w	2.526	12	2.530	0 2 4
vw	4.600*				w	2.422	9	2.426	2 3 2
mw	4.258	33	4.251	1 1 2	mw	2.305	11	2.304	2 0 4
w	3.961	9	3.961	0 2 2			5	2.256	2 1 4
vw	3.834				w	2.251	4	2.251	0 3 4
w	3.676	12	3.694	2 1 0	vw	2.185	1	2.182	3 2 2
		10	3.677	0 3 0	w	2.152	3	2.153	3 0 3
vw	3.592	1	3.589	0 1 3	w	2.091	5	2.097	2 4 2
w	3.504	10	3.514	2 1 1			4	2.005	3 2 3
w	3.416	6	3.416	1 0 3	vw	2.010	5	1.995	3 3 2
vw	3.345*				w	1.941	7	1.952	2 3 4
mw	3.195	27	3.196	2 2 0	w	1.824	4	1.822	2 5 2
mw	3.095	21	3.099	2 1 2	w	1.711	5	1.708	2 0 6

Notes: the d_{hkl} values were calculated on the basis of the unit-cell refined by using single-crystal data. Intensities ($I/I_{100} \times 100 > 1$ only) were calculated on the basis of the structural model. Observed intensities were visually estimated. vs = very strong; s = strong; ms = medium-strong; m = medium; mw = medium-weak; w = weak; vw = very weak. The * indicates three unindexed reflections, probably due to unidentified impurities.

498

499

500

501

502

503

504

505 **Table 3** – Crystal data and summary of parameters describing data collection and refinement for
 506 lusernaite-(Y).

507

Crystal data	
Crystal size (mm ³)	0.33 x 0.09 x 0.01
Cell setting, space group	Orthorhombic, <i>Pmna</i>
Unit-cell dimensions	
<i>a</i> (Å)	7.8412(3)
<i>b</i> (Å)	11.0313(5)
<i>c</i> (Å)	11.3870(4)
<i>V</i> (Å ³)	984.96(7)
<i>Z</i>	2
Data collection and refinement	
Radiation type, (λ)	Mo Kα (0.71073 Å)
Temperature (K)	~ 298
Maximum observed 2θ(°)	52.74
Measured reflections	23367
Unique reflections	1081
Reflections $F_o > 4\sigma F_o$	840
R_{int}	0.1131
$R\sigma$	0.0475
	$-9 \leq h \leq 9$
Range of <i>h</i> , <i>k</i> , <i>l</i>	$-13 \leq k \leq 13$
	$-14 \leq l \leq 14$
$R_1 [F_o > 4\sigma F_o]$	0.0682
R_1 (all data)	0.0861
wR_2 (on F_o^2)	0.1990
Goof	1.056
Number of I.s. parameters	90
$\Delta\rho_{max}$ and $\Delta\rho_{min}$	2.67, -1.09

Note: Extinction coefficient was 0. The weighting scheme is defined as $w = q/[\sigma^2(F_o^2) + (a^*P)^2 + b^*P]$, where $P = [2F_o^2 + \text{Max}(F_o^2, 0)]/3$.
 a and b values are 0.1419 and 2.9989.

508

509 **Table 4** – Atomic coordinates and displacement parameters for lusernaite-(Y).

510

Site	x/a	y/b	z/c	U_{11}	U_{22}	U_{33}	U_{23}	U_{13}	U_{12}	$U_{eq/iso}$
Y1	¼	0.4975(2)	¾	0.0120(7)	0.0281(13)	0.0111(7)	0	0.0007(4)	0	0.0170(6)
Pb1a	¼	0.570(7)	¾	0.0120(7)	0.0281(13)	0.0111(7)	0	0.0007(4)	0	0.0170(6)
Pb1b	¼	0.409(5)	¾	0.0120(7)	0.0281(13)	0.0111(7)	0	0.0007(4)	0	0.0170(6)
Y2	0	0.2304(1)	0.8487(1)	0.0166(8)	0.0282(9)	0.0160(8)	0.0001(6)	0	0	0.0203(6)
Al	0	½	0	0.012(3)	0.034(4)	0.009(3)	-0.002(2)	0	0	0.018(2)
C	½	0.683(1)	0.915(1)	0.016(8)	0.036(9)	0.012(7)	0.007(6)	0	0	0.021(3)
O1	-0.1624(9)	0.3949(7)	0.9272(6)	0.011(4)	0.046(5)	0.013(4)	-0.001(3)	0.001(3)	0.001(3)	0.023(2)
O2	0.357(1)	0.6424(8)	0.8746(7)	0.017(4)	0.054(6)	0.030(5)	-0.009(4)	0.007(3)	-0.007(4)	0.034(2)
O3	½	0.759(1)	0.9988(9)	0.022(6)	0.038(6)	0.018(5)	-0.011(4)	0	0	0.026(3)
O4	-¼	0.214(1)	¾	0.016(5)	0.046(7)	0.020(5)	0	0.000(3)	0	0.027(3)
O5	0	0.4177(9)	0.1437(8)	0.021(6)	0.033(6)	0.006(5)	0.007(4)	0	0	0.020(2)
O6	0	0.387(1)	0.7091(9)	0.019(6)	0.037(7)	0.007(5)	0.007(4)	0	0	0.021(2)
Ow1	-0.188(2)	0.135(1)	0.9854(9)	0.052(7)	0.063(7)	0.050(7)	0.019(5)	0.016(5)	0.007(6)	0.055(3)
Ow2	0	0.033(2)	0.770(2)	0.09(2)	0.10(2)	0.09(2)	-0.036(12)	0	0	0.093(7)
Ow3	-¼	-0.141(4)	¾							0.101(15)
H1	-0.201	0.037	0.989							0.05
H2	-0.314	0.158	0.014							0.05

511

512

513

514 **Table 5** – Selected bond distances (Å) for lusernaite-(Y).

Y1	– O2	2.297(8) × 2	Y2	– F4	2.267(1) × 2
	– O6	2.353(6) × 2		– O6	2.350(10)
	– O1	2.413(7) × 2		– Ow2	2.354(21)
	– O5	2.486(6) × 2		– Ow1	2.387(10) × 2
<Y1–O>		2.387		– O1	2.391(7) × 2
			<Y2–O>		2.349
Al	– O5	1.872(9) × 2	C	– O3	1.268(19)
	– O1	1.912(7) × 4		– O2	1.290(11) × 2
<Al–O>		1.898	<C–O>		1.28
			O2 – C – O3		119.8(7)°
			O2 – C – O2		120(1)°

515

516

517 **Table 6** – Bond-valence calculations for lusernaite-(Y), according to Brese and O’Keeffe (1991).

	Y1	Y2	Al	C	Σv (O-X)	Σv (O-X)*	species
518 O1	0.34 ^a	0.36 ^a	0.49 ^b		1.19	0.99	OH ⁻
519 O2	0.47 ^a			1.31 ^a	1.78	1.98	O ²⁻
520 O3				1.39	1.39	2.13**	O ²⁻
521 O4		0.46 ^a			0.92	0.92	OH ⁻ , F ⁻
522 O5	0.28 ^a		0.55 ^a		1.11	1.11	OH ⁻
523 O6	0.40 ^a	0.40			1.20	1.04	OH ⁻
524 Ow1		0.36 ^a			0.36	0.01***	H ₂ O
525 Ow2		0.40			0.40	0.27****	H ₂ O
526 Ow3					0.00	0.60	OH ⁻
						-0.15	H ₂ O
527 Σv (X-O)	2.98	3.16	3.06	4.01			

527 ^a(2 X →). ^b(4 X →). *Bond valence balance after correction for O...O hydrogen bonds.
 528 **If involved in Ow3...O2 hydrogen bond. ***If donor in Ow1...Ow1 hydrogen bond. ****If
 529 acceptor in Ow1...Ow1 hydrogen bond. For Y1 and Y2 sites, the parameters for Y-O and
 530 Y-F bonds were used.
 531

532 **Table 7** – O···O distances (in Å) in the suggested hydrogen-bonding scheme, with corresponding
533 bond-valence values (*vu*).
534

O···O bond donor → acceptor	d (Å)	<i>vu</i>
Ow1 (H ₂ O) → O3 (O)	2.72(1)	0.22
Ow2 (H ₂ O/OH) ↔ Ow3 (H ₂ O)	2.75(4)	0.20
O1 (OH) → O2 (O)	2.76(1)	0.20
O6 (OH) → O3 (O)	2.89(2)	0.16
Ow3 (H ₂ O) → O2(O)	2.91(4)	0.15
Ow1 (H ₂ O) ↔ Ow1 (H ₂ O)	2.99(2)	0.13

535

536 **Table 8** – Comparison of natural yttrium carbonates.

	Chemical formula	<i>a</i> (Å)	<i>b</i> (Å)	<i>c</i> (Å)	α (°)	β (°)	γ (°)	S.G.	Ref.
5.B Carbonates with additional anions, without H₂O									
bastnäsite-(Y)	(Y,REE)(CO ₃)F	6.57	6.57	9.48	90	90	120	<i>P6</i>	[1]
horváthite-(Y)	NaY(CO ₃)F	6.96	9.17	6.30	90	90	90	<i>Pmcn</i>	[2]
mineevite-(Y)	Na ₂₅ Ba(Y,Gd,Dy) ₂ (CO ₃) ₁₁ (HCO ₃) ₄ (SO ₄)F ₂ Cl	8.81	8.81	37.03	90	90	120	<i>P6₃/m</i>	[3]
reederite-(Y)	Na ₁₅ Y ₂ (CO ₃) ₉ (SO ₃ F)Cl	8.77	8.77	10.75	90	90	120	<i>P-6</i>	[4]
synchysite-(Y)	Ca(Y,Ce)(CO ₃) ₂ F	12.04	6.95	18.44	90	102.45	90	<i>C2/c</i>	[5]
5.C Carbonates without additional anions, with H₂O									
adamsite-(Y)	NaY(CO ₃) ₂ ·6H ₂ O	6.26	13.05	13.22	91.17	103.70	89.99	<i>P-1</i>	[6]
donnayite-(Y)	NaCaSr ₃ Y(CO ₃) ₆ ·3H ₂ O	9.00	9.00	6.79	102.77	116.28	59.99	<i>P1</i>	[7]
hizenite-(Y)	Ca ₂ Y ₆ (CO ₃) ₁₁ ·14H ₂ O	6.30	9.09	63.49	90	90	90	UK	[8]
								<i>Imm2</i>	
kimuraite-(Y)	CaY ₂ (CO ₃) ₄ ·6H ₂ O	9.25	23.98	6.04	90	90	90	<i>Immm</i> <i>I222</i>	[9]
								<i>I2₁2₁2₁</i>	
lecoqite-(Y)	Na ₃ Y(CO ₃) ₃ ·6H ₂ O	11.32	11.32	5.93	90	90	120	<i>P6₃</i> <i>Pb2m</i>	[10]
lokkaite-(Y)	CaY ₄ (CO ₃) ₇ ·9H ₂ O	39.07	6.08	9.19	90	90	90	<i>Pbm2</i> <i>Pbmm</i>	[11]
mckelveyite-(Y)	NaCa(Ba,Sr) ₃ (Y,REE)(CO ₃) ₆ ·3H ₂ O	9.17	9.17	9.15	90	90	90	<i>P-3</i>	[12]
shomiokite-(Y)	Na ₃ Y(CO ₃) ₃ ·3H ₂ O	10.04	17.32	5.94	90	90	90	<i>Pbn2₁</i>	[13]
tengerite-(Y)	Y ₂ (CO ₃) ₃ ·2·3H ₂ O	6.08	9.16	15.11	90	90	90	<i>Bb2₁m</i>	[14]
5.D Carbonates with additional anions, with H₂O									
								<i>P2</i>	
decrepignyite-(Y)	(Y,REE) ₄ Cu(CO ₃) ₄ Cl(OH) ₅ ·2H ₂ O	8.90	22.77	8.59	90	120.06	90	<i>Pm</i> <i>P2/m</i>	[15]
kamphaugite-(Y)	Ca(Y,REE)(CO ₃) ₂ (OH)·H ₂ O	7.43	7.43	21.79	90	90	90	<i>P4₁2₁2</i>	[16]
lusernaite-(Y)	Y ₄ Al(CO ₃) ₂ (OH,F) ₁₁ ·6H ₂ O	7.84	11.03	11.39	90	90	90	<i>Pmna</i>	[17]
thomasclarkite-(Y)	(Na,Ce)(Y,REE)(HCO ₃)(OH)3·4H ₂ O	4.56	13.02	4.56	90	90.15	90	<i>P2</i>	[18]
5.E Uranyl carbonates									
bijvoetite-(Y)	(Y,Dy) ₂ (UO ₂) ₄ (CO ₃) ₄ (OH) ₆ ·11H ₂ O	21.23	12.96	44.91	90	90	90	<i>B2₁</i>	[19]
kamotoite-(Y)	Y ₂ U ₄ (CO ₃) ₃ O ₁₂ ·14.5H ₂ O	21.22	12.93	12.39	90	115.3	90	<i>P2₁/n</i>	[20]

[1] Mineev et al. 1970; [2] Grice and Chao 1997; [3] Khomyakov et al. 1992; [4] Grice et al. 1995; [5] Wang and Zhou 1995; [6] Grice et al. 2000; [7] Chao et al. 1978; [8] Takai and Uehara 2011; [9] Nagashima et al. 1986; [10] Pekov et al. 2010; [11] Perttunen 1970; [12] Milton et al. 1965; [13] Grice 1996; [14] Miyawaki et al. 1993; [15] Wallwork et al. 2002; [16] Raade and Brastad 1993; [17] this work; [18] Grice and Gault 1998; [19] Li et al. 2000; [20] Deliens and Piret 1986. UK = unknown space group.

537

538

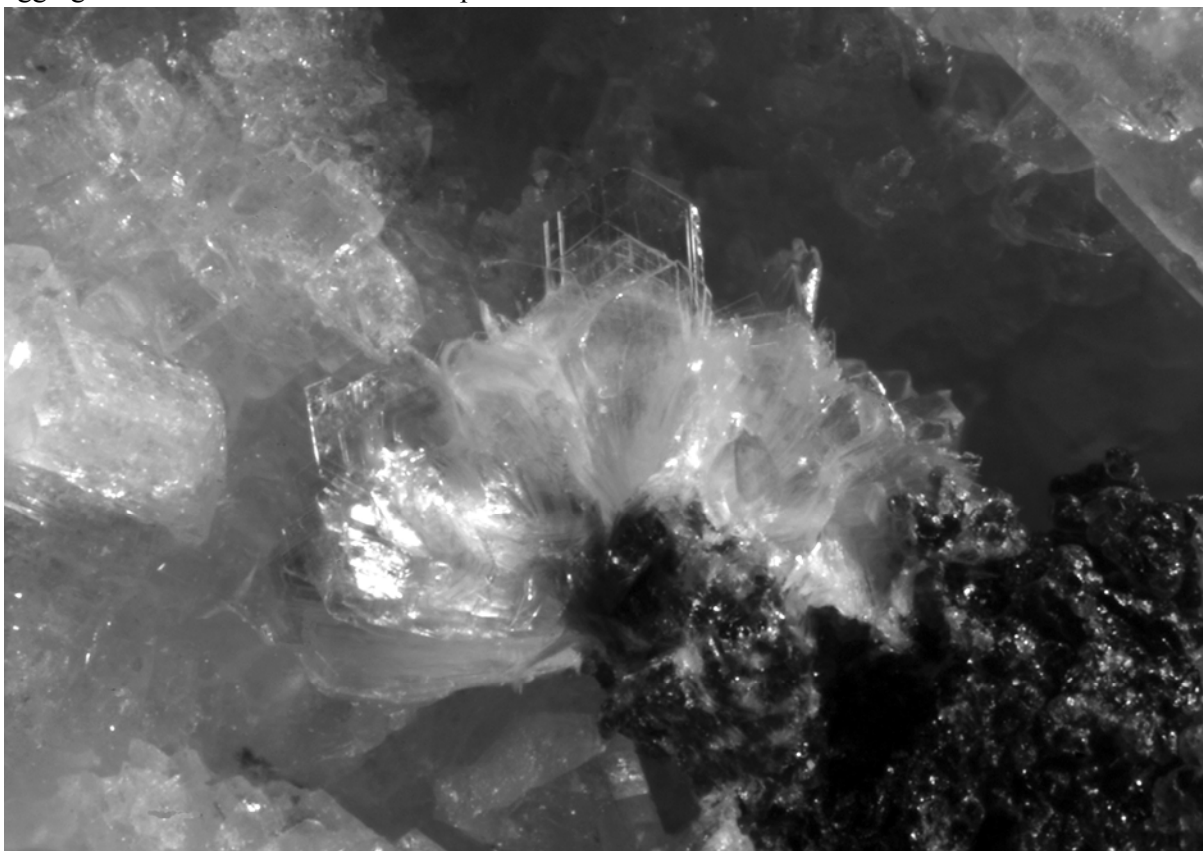
539

540

541

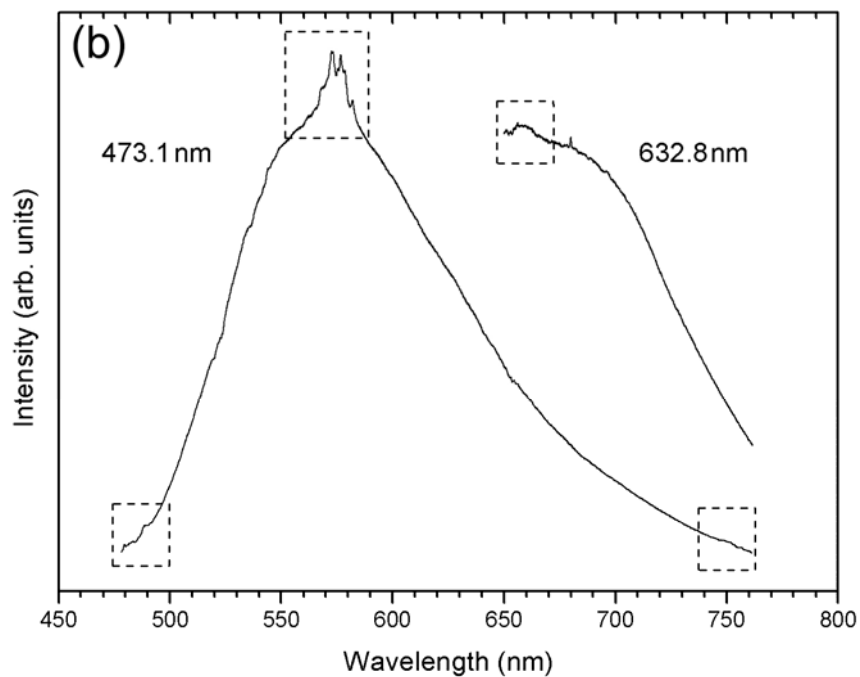
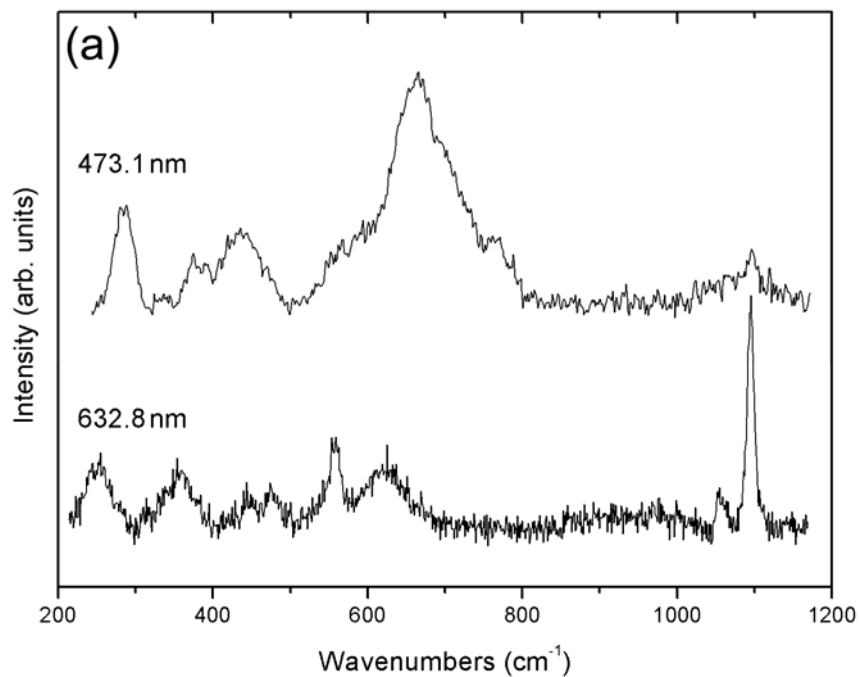
542

543 **Figure 1** – Colourless thin tabular crystals of lusernaite-(Y) associated with “chlorite”. Crystal
544 aggregate size: 2 mm. Collection and photo B. Marello.



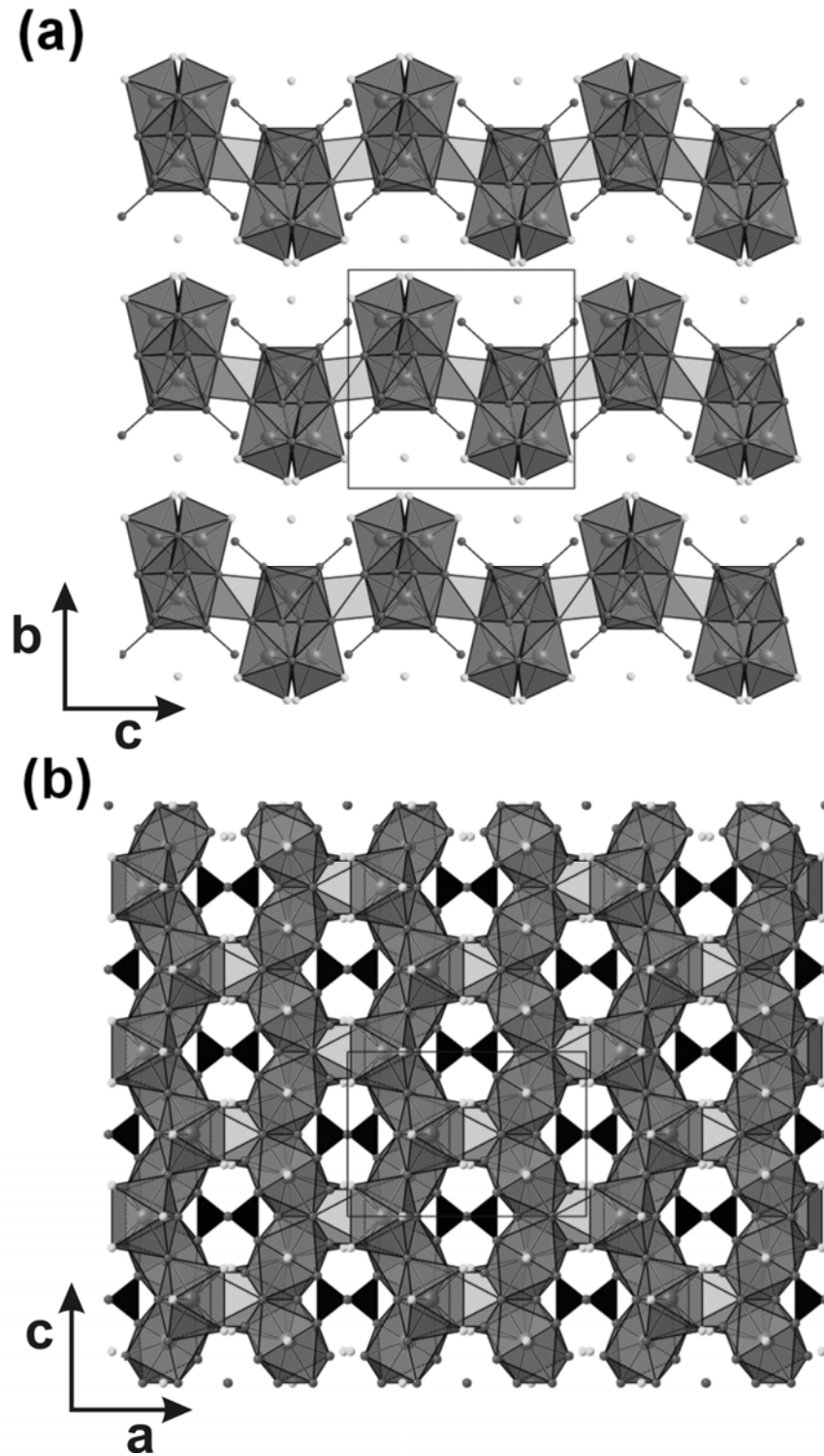
545
546

547 **Figure 2** – Micro-Raman spectra of lusernaite-(Y) between 200 and 1200 cm^{-1} (a) and the effect of
548 luminescence (b) for both 473.1 and 632.8 nm excitation lines.



549
550
551

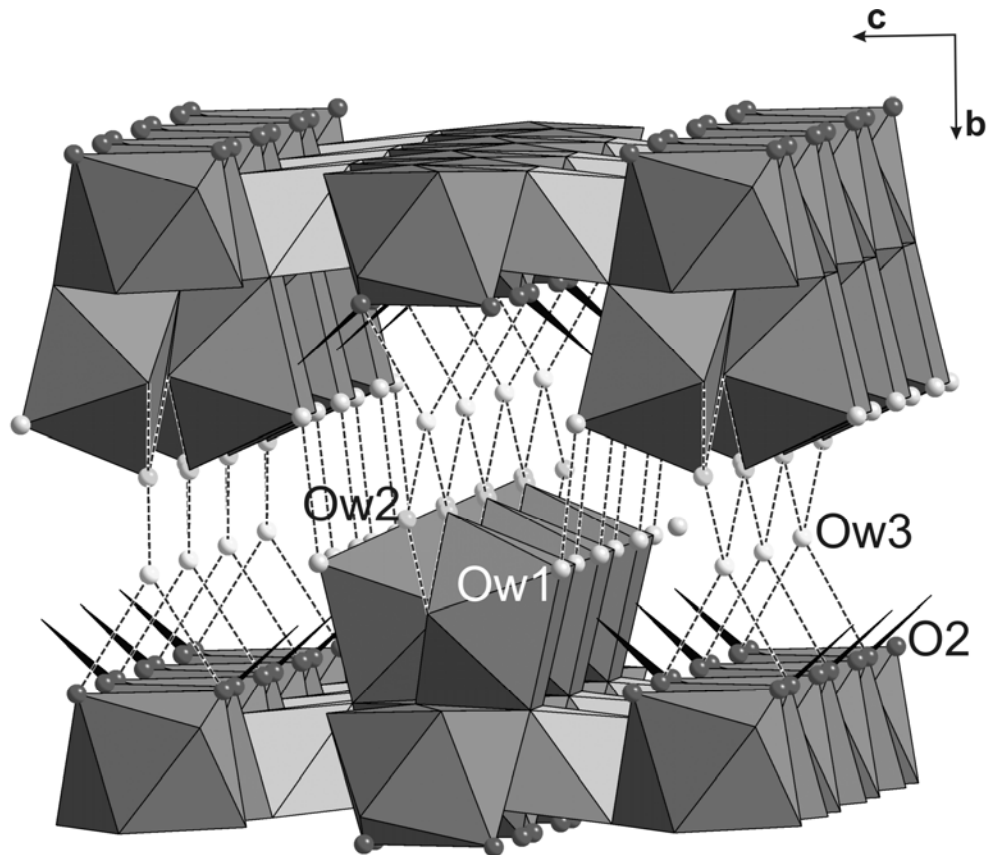
552 **Figure 3** – Crystal structure of lusernaite-(Y), as seen down [100] (a) and [010] (b). Polyhedra: dark
553 grey = Y-centered polyhedra; light grey = Al-centered octahedra; black = CO₃ groups. Balls: dark
554 grey = O²⁻ or (OH,F)⁻ anions; light grey = H₂O molecules or mixed H₂O/OH⁻ occupied site.
555



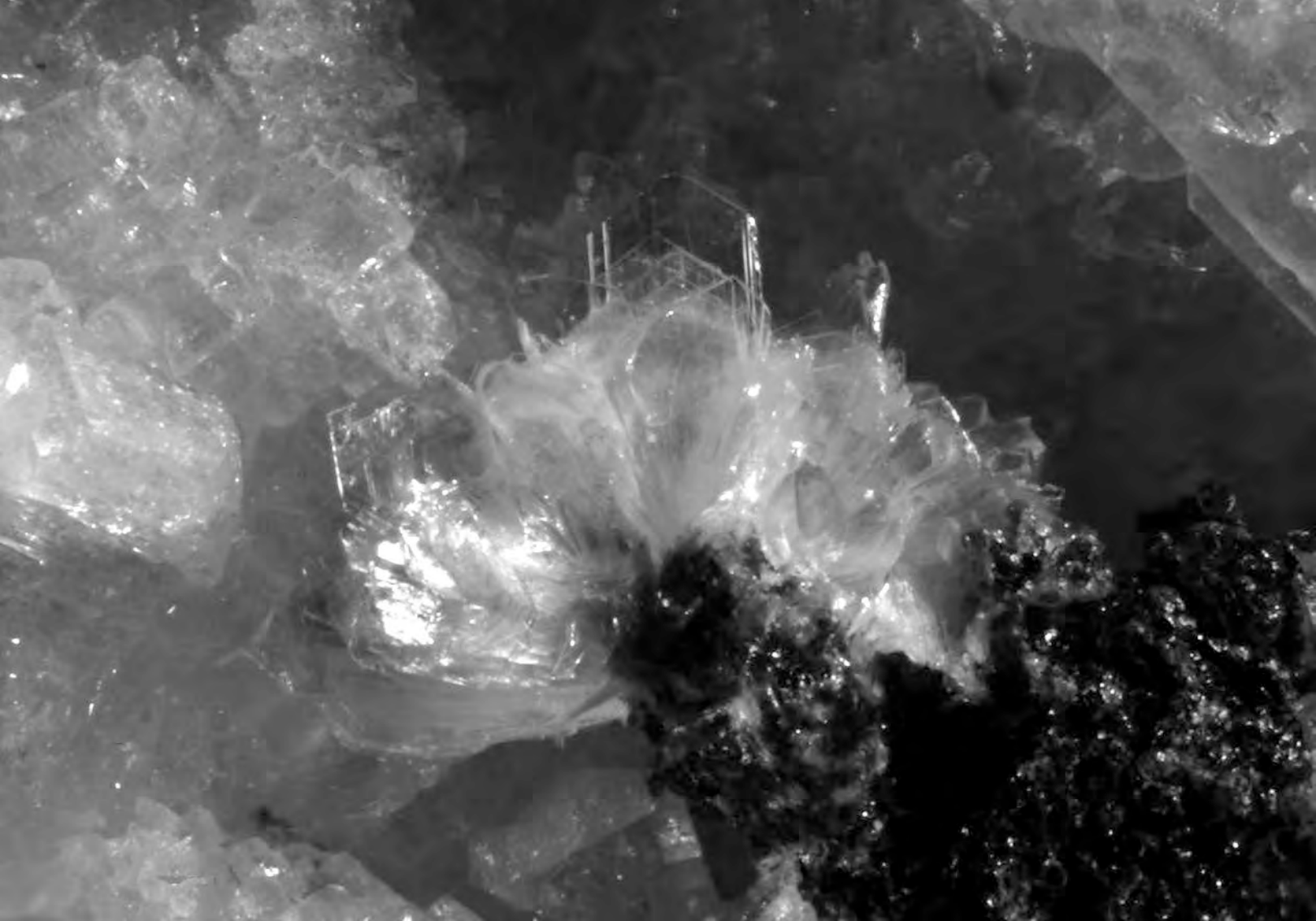
556
557

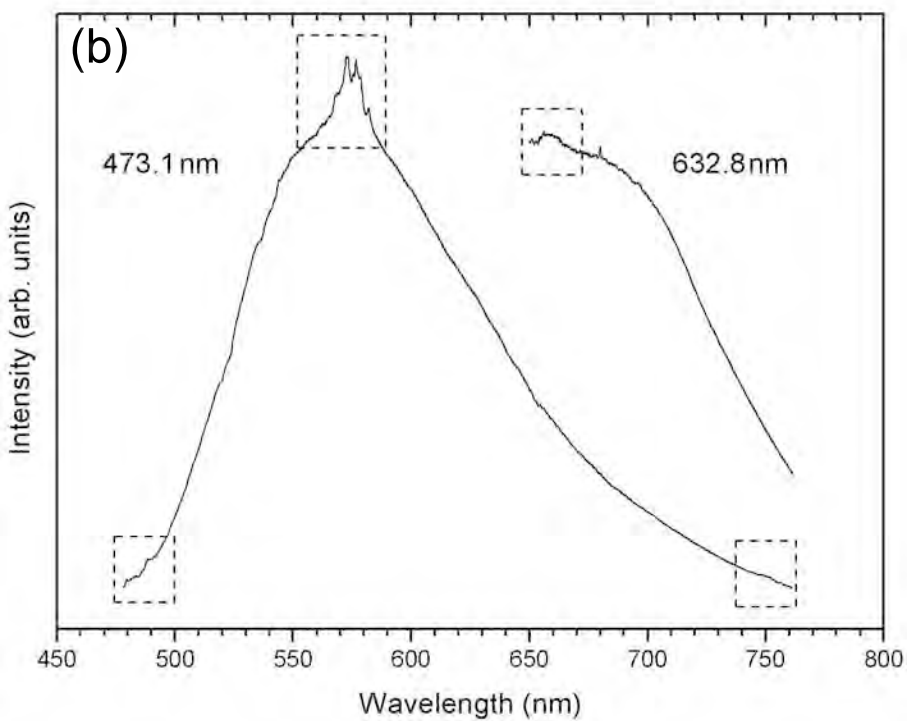
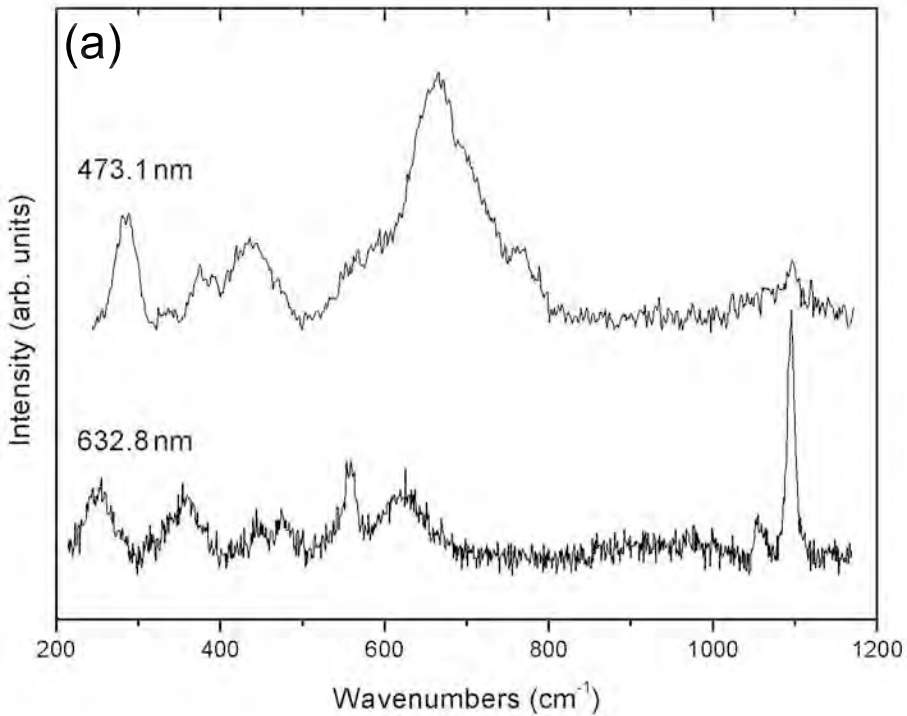
558

559 **Figure 4** – The possible hydrogen bonds connecting successive (010) layers. Polyhedra: dark grey:
560 Y-centered polyhedra; light grey: Al-centered octahedra; black = CO₃ groups. Balls: dark grey: O2
561 sites; grey: Ow1, Ow2, Ow3 sites.

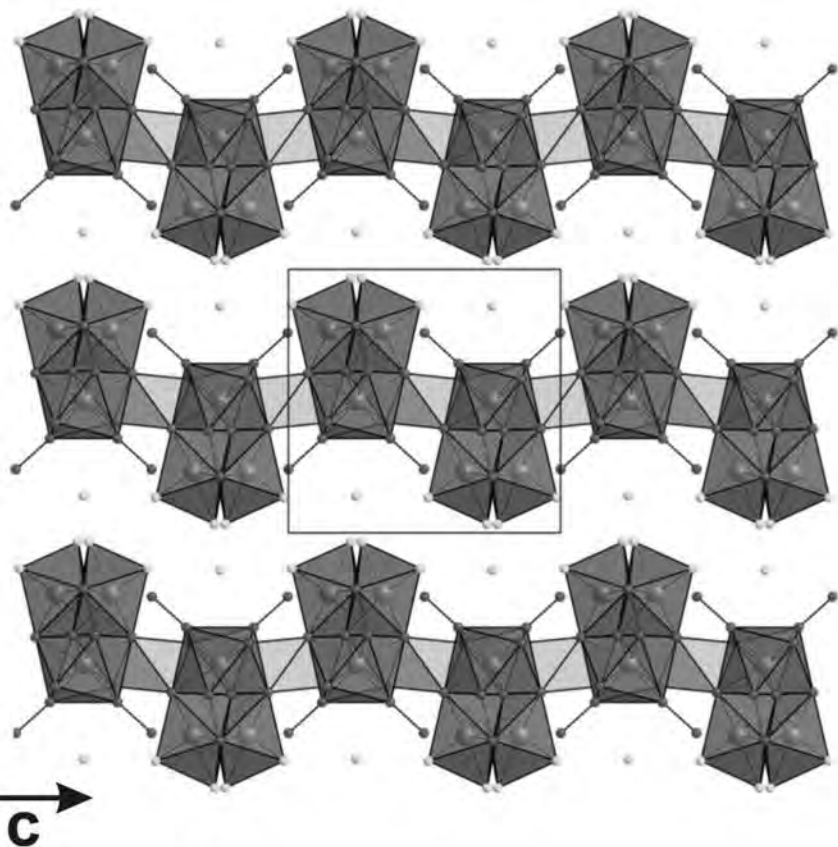


562





(a)



(b)

